Computational Materials Science 44 (2008) 296–302

Contents lists available at ScienceDirect

Computational Materials Science

journal homepage: www.elsevier.com/locate/commatsci

Mathematical model for a straight grate iron ore pellet induration process of industrial scale

S.K. Sadrnezhaad *, A. Ferdowsi, H. Payab

Materials and Energy Research Center, P.O. Box 14155-4777, Tehran, Iran
Center of Excellence for Advanced Processes of Production of Materials, Department of Materials Science and Engineering, Sharif University of Technology, P.O. Box 11365-9466, Tehran, Iran

A R T I C L E I N F O

Article history:
Received 1 April 2007
Received in revised form 7 March 2008
Accepted 19 March 2008
Available online 9 May 2008

Keywords:
Mathematical modeling
Straight grate
Induration process
Iron ore pellet
Fuel consumption
Greenhouse gases

A B S T R A C T

A mathematical model is developed for induration of the iron-ore pellets in an industrial-scale plant based on the laws of mass, heat and momentum transfer. Physicochemical processes occurring during the induration of pellets such as drying of moisture, calcination of limestone and coke-magnetite reaction are considered to evaluate the gradient of temperature within the pellets. Differential equations describing transport phenomena in a grate bed are simultaneously solved by dividing the space in both *x*- and *z*- directions and numerically solving the phenomenological equations. A kinetic model is used for estimation of the change of the strength of the pellets due to firing. The model involves gas-flow through different zones of a typical industrial plant. Different conditions are used for determination of the effect of addition of carbon to the green pellets on performance of the induration process. The optimum carbon content is determined to be 0.75% for green pellets. This results in a productivity enhancement of 20%, an N.G. fuel consumption decrease of 17% and an electrical power saving of 17%. Based on the model calculations, the volumes of the wasted greenhouse gases diminish with addition of the carbon content of the pellets.

1. Introduction

Pelletizing is a common process used usually for upgrading of the iron-ore raw fines [1]. Green pellets are made of concentrates continuously rolled over in rotary discs with moisture, bentonite, limestone, coke breeze, etc. These pellets are loaded onto a traveling grate where they are dried and fired to increase their strength. They form a packed-bed that is subsequently air-cooled to recycle the heat and to obtain an appropriate temperature for further handling.

Two types of systems are usually used for induration of the iron-ore pellets: (a) straight-grate and (b) grate-kiln process. A hearth layer of fired pellets is used in the former to protect grate bars from excessive heating. Fresh pellets are charged onto a hearth layer of the fired ones. Hot gas is blown through the layer to dry-out and fire the pellets at about 1300 °C. In the grate-kiln process, the green pellets are charged onto the grate to form a bed of ~180 mm depth. In this process, the bottom of the bed does not heat-up so much to damage the grate bars. No hearth layer is, therefore, required in this process. Pellets charged onto the grate are subject to up-draft drying, down-draft drying and preheating with streams of the gases. The pellets discharged onto the rotary kiln furnace are fired and then transferred into the annular cooler to form a deep-packed bed. Ambient air is blown through the bed to abstract heat from the pellets.

This article focuses on the straight grate type of the pellet induration process. In industrial plants, the moving grate is divided into several zones such as those of KSC (Kouzestan Steel Company of Iran) shown in Fig. 1: (a) up-draft drying (UDD); (b) down-draft drying (DDD); (c) preheating (PH); (d) first firing (F1); (e) second firing (F2) (f) after-firing (AF); (g) first cooling (C1) and (h) second cooling (C2) zones. In drying zones, gas stream is used to dry the pellets at 200–300 °C. That why most processes use a combination of up-draft/down-draft drying is for prevention of decrepitation of the pellets under a combination of the gravity forces, the pressure drop generated to pull back the gases trough the bed and the moisture re-condensation process.

Off-gases of the second cooling stage are used in the drying zone. This zone does not have any burner. In PH, F1 and F2 zones,

* Corresponding author. Address: Center of Excellence for Advanced Processes of Production of Materials, Department of Materials Science and Engineering, Sharif University of Technology, P.O. Box 11365-9466, Tehran, Iran, Tel.: +98 2166165215; fax: +98 2166005717.
E-mail addresses: sadrnezh@sharif.edu, sadrnezh@yahoo.com (S.K. Sadrnezhaad).

0927-0256/$ - see front matter © 2008 Elsevier B.V. All rights reserved.
doi:10.1016/j.commatsci.2008.03.024

Nomenclature

A	surface area of pellets per m^3 pellet bed ($m^2\ m^{-3}$)
C_g, C_s	heat capacity of gas, pellets ($J\ kg^{-1}\ K^{-1}$)
C_i	concentration of component i ($mol\ m^{-1}$)
D_i	diffusion coefficient of component i ($m^2\ s^{-1}$)
d	pellet diameter (m)
G	gas flow rate ($kg\ m^{-2}\ s^{-1}$)
h	convection heat transfer coefficient ($J\ m^{-2}\ s^{-1}\ K^{-1}$)
k	thermal conductivity of pellet ($J\ m^{-1}\ K^{-1}\ s^{-1}$)
K_l	equilibrium constant of limestone reaction (atm)
k_g	mass transfer coefficient ($m\ s^{-1}$)
k_l, $k_{r,c}$, $k_{r,m}$	chemical reaction rate of limestone, carbon, magnetite ($m\ s^{-1}$)
M	superficial pellet flow ($kg\ m^2\ s^{-1}$)
$\dot{m}$	mass flow of gas ($kg\ s^{-1}$)
P	pressure (Pa)
r_0	radius of pellet (m)
r	distance from the center of pellet (m)
r_w r_m, r_l, r_c	radius of moisture, magnetite, limestone, carbon core (m)
R	gas constant ($m^3\ atm\ K^{-1}$)
R_i	reaction rate of component i ($mol\ m^{-3}\ s^{-1}$)
t	time (s)
T_g, T_p	temperature of gas, pellet (°C)
T_p^s	surface temperature of pellet (°C)
W_g, W_g^{eq}	gas humidity ($kg\ m^{-3}$)
W_p, W_{pc}	pellet humidity ($kg\ m^{-3}$)
x	length in furnace (m)
z	bed height (m)
ΔH_i	enthalpy of reaction of the component i of the pellet ($J\ kg^{-1}$)
ΔH_v	enthalpy of vaporization of the moisture of the pellet ($J\ kg^{-1}$)
φ	void fraction of pellet bed
μ	viscosity ($kg\ m^{-1}\ s^{-1}$)
ρ_g, ρ_p	density of gas, pellet ($kg\ m^{-3}$)

off-gases of the first cooling zone are heated under burner hoods to raise their temperatures up to about 800, 1200 and 1300 °C, respectively. Since the AF zone has no burner, the off-gases coming from C1 zone having a temperature of ~1000 °C is directly employed to stabilize the temperature of the bed. Energy consumption by the induration machine is, thus, related to the performance of the cooling zones [2].

Due to the high energy consumption, the induration of the iron ore pellets is a relatively expensive process. Empirical studies have so far been made to optimize the operation with respect to both fuel efficiency and materials productivity [3–5]. Strong coupling effects of the counter-current gas and solid materials moving through the system makes the mathematics more confusing to be treated in a traditional way [6–8]. Assessment of the effect of an individual change even if it is too small and takes place at a specific location is not too simple. Application of a trial and error technique for identification of the concentration, temperature and velocity profiles of the solid materials moving on the grate is expensive especially with poor quality pellets. Results depend on the specific machine used and the operational conditions.

For induration of the iron-ore pellets, a number of models have been presented in the literature [2,6,7,9–15]. Hasenack et al. [9] and Voskamp and Brasz [10] have presented the first models. Thurlby [3,11,12] and Young et al. [13] have proposed models devoted to the grate-kiln systems. Thurlby et al. [14] have developed a model for the moving grate iron-ore induration of the pellets. A mathematical model for a pilot scale induration furnace for iron-ore pellets has been presented by Kucukada et al. [15]. Cross and Blot [6] have used the induration process model to evaluate the suitability of the first drying zone with the updraft or downdraft gas flow streams. They have optimized the gas temperature profile in the hood of PH, F, and AF zones to reduce the burner fuel. Hamidi and Payab [7] have presented a mathematical model for pilot-scale iron ore induration furnace and have determined energy savings by coke addition to the pellet and oxygen injection to the furnace. Pomerleau et al. [16] have used a mathematical model for optimization of the operating conditions in a straight grate furnace. They have discussed the conditions for decrease of the fuel consumption and increase of the production rate.

The present study utilizes a more sophisticated model than those developed before by considering (a) gas-composition variation along the bed of the pellets, (b) changing of the gas-concentration from one stage to the other, (c) temperature gradient within the pellets and (d) industrial scale geometry for simulation of the induration process. The model is eventually assessed by application the industrial data obtained from KSC plant being currently operated for production of the iron ore pellets.

2. Modeling

Thurlby et al. [14] have comparatively examined the effect of radiation and found that its effect is negligible. Mitterlehner et al. [17], Pomerleau et al. [5] and other investigators have, therefore, ignored the radiation in their plant simulation. Because of the small difference between the gas and wall temperatures, this seems to be a valid assumption and therefore transfer of heat by radiation and within the bed can be neglected. The process is assumed to occur at the steady state. The model includes drying of the pellets and reactions of the limestone, magnetite and carbon being contained in the pellets.

2.1. Energy balance

To model the iron-ore induration process, let's assume that the bed voidage and height during sintering is constant. Consider a cell having the height dz and ignoring the change of gas temperature with time, the gaseous phase energy balance can be written as[1]

$$\frac{\partial(GC_gT_g)}{\partial z} + ha(T_g - T_p^s) = 0 \tag{1}$$

The energy balance for the same cell with a length dx is

$$-\frac{\partial(MC_sT_s)}{\partial x} + ha(T_g - T_p^s) - (1-\varepsilon)\Delta H_v\frac{dW_p}{dt} + \sum(1-\varepsilon)R_i\Delta H_i = 0 \tag{2}$$

It has previously been reported that the temperature gradient within the pellets plays an important role in the determination of the minimum firing time [1]. Since the heat transfer within the pellets takes place by conduction, the energy balance for an individual pellet can be expressed by the following equation [18]:

[1] All symbols are given in Nomenclature.

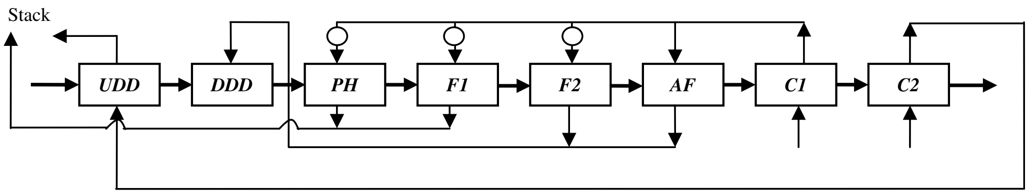

Fig. 1. Schematic diagram of a straight grate induration furnace.

$$k\frac{1}{r^2}\frac{\partial}{\partial r}\left(r^2\frac{\partial T_\mathrm{p}}{\partial r}\right)+\sum \Delta H_i R_i+\Delta H_\mathrm{v}\left(\frac{\mathrm{d}W_\mathrm{p}}{\mathrm{d}t}\right)=\rho_\mathrm{p} C_\mathrm{p}\frac{\partial T_\mathrm{p}}{\partial t} \tag{3}$$

B.C.1: $k\frac{\partial T_\mathrm{p}}{\partial r}\Big|_{r=d/2}=h(T_\mathrm{g}-T_\mathrm{p})$B.C.2: $\frac{\partial T_\mathrm{p}}{\partial r}\Big|_{r=0}=0$ In this equation a homogeneous pore/different-phases distribution is assumed for the pellets. An average conductivity consisting of pore, different phases and chemical compounds is estimated for mathematical evaluations. These assumptions have been used also by previous investigators [15]. After determining the temperature of the pellet as a function of its radius, average temperature of the pellet Ts, can be calculated by Eq. (4) [16]

$$T_\mathrm{s}=\frac{\int_0^{d/2}4\pi r^2 T_\mathrm{p}(r)\,\mathrm{d}r}{\int_0^{d/2}4\pi r^2\,\mathrm{d}r} \tag{4}$$

2.2. Evaporation

It is postulated that the moisture evaporation takes place at the pellet surface until its content drops below a critical humidity, above which there is a continuous water movement to the pellet surface by capillary forces to keep the surface saturated with water. When the moisture content reaches to a critical level, the pellet is assumed to be formed of a dry shell and a wet core separated by an inward moving front. Critical wet-core humidity remains constant and the outskirts water continues to evaporate. Critical humidity depends on the physico-chemical nature of a pellet, irrespective of the temperature [1]. With heating of the pellets, the evaporation process can take place; while no considerable change occurs in the temperature of the pellets.

The drying of an iron ore pellet can thus be represented by the following two resistance model:

$$-(1-\varepsilon)\frac{\mathrm{d}W_\mathrm{p}}{\mathrm{d}t}=\frac{a}{(d/2)^2}\,\frac{(W_\mathrm{g}^\mathrm{e}-W_\mathrm{g})}{\frac{d/2-r_\mathrm{w}}{(d/2)r_\mathrm{w}D_{\mathrm{H_2O}}}+\frac{1}{k_{\mathrm{g,H_2O}}(d/2)^2}} \tag{5}$$

The wet core radius, r_w, pellet diameter, d, pellet humidity, W_p, and critical humidity of pellets, W_pc, can be related together by the following water mass balance equation:

$$W_\mathrm{p}=W_\mathrm{pc}\left(\frac{r_\mathrm{w}}{d/2}\right)^3 \tag{6}$$

Specific consideration is required for the beginning of the drying cycle when the air comes into contact with the pellets at a lower temperature than the temperature of the saturated air.

2.3. Chemical reactions

At least three reactions take place within the hot pellets. Three controlling steps (film diffusion, pore diffusion and chemical reaction) are considered by previous authors to control the rate of the reactions according to the shrinking core regime [13]

$$\mathrm{CaCO_3(s)=CaO(s)+CO_2(g)}$$

$$R_\mathrm{lim}=\frac{4\pi r_0^2(C_{\mathrm{CO_2}}^{\mathrm{eq}}-C_{\mathrm{CO_2}})}{\frac{1}{k_{\mathrm{g(CO_2)}}}+\left[\frac{r_0}{r_l(t)}\right]^2\frac{K_1}{k_1RT_\mathrm{s}}+\frac{r_0[r_0-r_1(t)]}{r_1(t)D_{\mathrm{CO_2}}}} \tag{7}$$

$$\mathrm{4Fe_3O_4(s)+O_2(g)\rightarrow 6Fe_2O_3(s)}$$

$$R_\mathrm{mag}=\frac{16\pi r_0^2(C_{\mathrm{O_2}}^{\mathrm{eq,m}}-C_{\mathrm{O_2}})}{\frac{1}{k_{\mathrm{g(O_2)}}}+\left[\frac{r_0}{r_\mathrm{m}(t)}\right]^2\frac{1}{k_\mathrm{r,m}}+\frac{r_0[r_0-r_\mathrm{m}(t)]}{r_\mathrm{m}(t)D_{\mathrm{O_2}}}} \tag{8}$$

$$\mathrm{C(s)+O_2(g)\rightarrow CO_2(g)}$$

$$R_\mathrm{car}=\frac{4\pi r_0^2(C_{\mathrm{O_2}}-C_{\mathrm{O_2}}^{\mathrm{eq,c}})}{\frac{1}{k_{\mathrm{g(O_2)}}}+\left[\frac{r_0}{r_\mathrm{c}(t)}\right]^2\frac{1}{k_\mathrm{r,c}}+\frac{r_0[r_0-r_\mathrm{c}(t)]}{r_\mathrm{c}(t)D_{\mathrm{O_2}}}} \tag{9}$$

2.4. Gas flow

During the induration process, the rate of flow of the gases changes from one zone to the other. Pressure drop remains, however, constant across the bed of the pellets at a value specified by each of the drying, firing and cooling subsystems. The Ergun's equation can be used to evaluate the gas flow rate for a given pressure drop [18]

$$-\frac{\mathrm{d}P}{\mathrm{d}z}=\frac{150(1-\varepsilon)^2\mu}{d^2\varepsilon^3\rho_\mathrm{g}}G+\frac{1.75(1-\varepsilon)}{d\varepsilon^3\rho_\mathrm{g}}G^2 \tag{10}$$

2.5. Mass balance

Because of evaporation of the moisture contained in the pellets, decomposition of limestone according to Reaction 7 and oxidation of magnetite according to Reaction 8 and oxidation of carbon according to Reaction 9, composition of the gaseous phase changes during the induration process. Mass balances written for water, oxygen and carbon dioxide are as follows:

$$-\frac{\partial}{\partial z}(GW_\mathrm{g}/GW_\mathrm{g}\rho_\mathrm{g})-(1-\varepsilon)\frac{\mathrm{d}W_\mathrm{p}}{\mathrm{d}t}=0 \tag{11}$$

$$-\frac{\partial}{\partial z}(GC_{\mathrm{O_2}}GC_{\mathrm{O_2}}\rho_\mathrm{g}\rho_\mathrm{g})-(1-\varepsilon)R_\mathrm{c}-(1-\varepsilon)R_\mathrm{m}=0 \tag{12}$$

$$-\frac{\partial}{\partial z}(GC_{\mathrm{CO_2}}/GC_{\mathrm{CO_2}}\rho_\mathrm{g}\rho_\mathrm{g})+(1-\varepsilon)R_\mathrm{c}+(1-\varepsilon)R_\mathrm{m}=0 \tag{13}$$

The above differential equations are solved by using explicit finite difference method to evaluate the temperatures of the pellets and gases at different bed heights during the induration process.

2.6. Fuel-gas consumption

Both temperature and composition of the inlet gases are determined in order to solve the equations describing the state of the bed of the pellets. These parameters depend on the processes occurring elsewhere. Fig. 1 shows the inter-effect between different zones of the straight grate furnace used in KSC. This furnace uses natural gas as its fuel. Mass and energy balances established between different zones must be developed to obtain temperature and composition of the inlet gases. Mass balance for the *Firing* zone can for example be written as follows:

$$\dot{m}_{\mathrm{F}} = \dot{m}_{C1\rightarrow F} + \dot{m}_{\mathrm{air}} + \dot{m}_{\mathrm{N.G.}} \tag{14}$$

Energy balance for the *firing* zone can also be written as follows:

$$\int_{T_{C1}}^{T_{\mathrm{F}}} \dot{m}_{C1}.c_{p,C1}\,\mathrm{d}T + \int_{T_{\mathrm{air}}}^{T_{\mathrm{F}}} \dot{m}_{\mathrm{air}}.c_{p,\mathrm{air}}\,dT + \int_{T_{\mathrm{N.G.}}}^{T_{\mathrm{F}}} \dot{m}_{\mathrm{N.G.}}.c_{p,\mathrm{N.G.}}\,dT = 0 \tag{15}$$

2.7. Estimation of pellet quality

The fired strength of the heat-hardened iron ore pellets may also be predicted by the mathematical model developed in this research. Batterham [19] presented formalism for strength development in the pellets that involves no restriction on the form of the applied time-temperature curve:

$$\frac{\mathrm{d}Q}{\mathrm{d}t} = f(Q,T) = \psi(Q_{\mathrm{f}} - Q) \tag{16}$$

The temperature dependent rate parameter, ψ, can be represented by an Arrhenius type expression:

$$\psi = \frac{A_0}{T}\exp\left(\frac{-E}{RT}\right) \tag{17}$$

In order to define an appropriate form of Q_{f} (the final quality that would be attained after a long period of sintering at temperature T), it is necessary to account for rapid rise in the fired quality that occurs once T exceeds a specified value T_0. A suitable form is

$$\begin{aligned} &Q_{\mathrm{f}} = \alpha + \beta(T - T_0) \quad T > T_0 \\ &Q_{\mathrm{f}} = \alpha \quad T \leqslant T_0 \end{aligned} \tag{18}$$

The final equation has, therefore, five adjustable parameters: A_0, E, α, β and T_0. These parameters vary with the nature and amount of the additives, the ore-type and the balling conditions. Once these parameters are determined, the state equation can be used to integrate along any time-temperature profile by solving

$$Q_{\mathrm{p}} = \int_0^t \frac{\mathrm{d}Q}{\mathrm{d}t}\,\mathrm{d}t \tag{19}$$

where Q_{p} is the product quality at the end of the induration process. The model developed does not consider decreasing of the pellet quality that occurs above a critical temperature due to verification phenomenon. Although the quality parameter Q_{p} has industrially been unspecified, the JIS abrasion index AI, is commonly used. The quality parameter is related to the abrasion index according to the following equation:

$$Q_{\mathrm{p}} = \frac{100 - \mathrm{AI}}{\mathrm{AI}} \tag{20}$$

3. Results and discussion

Thermal profile of a pellet during induration process is the most important factor that can assure the quality of the fired pellets. Although the temperature of the enduring bed of the pellets has not so far been measured [2], the temperature of the gases at different heights can be used to assess the simulation results. Fig. 2 compares the experimental and the simulated temperature profiles of the gas at different heights for a complete pellet induration sequence. Pellet-temperature profiles calculated in this work are compared with those of previous investigators in Fig. 3 [10,13].

The amount of the energy consumed by an induration furnace and the quality of the fired pellets are two important factors that need to be treated by the model developed. The amounts of the N.G. that burns in the furnace and the abrasion index of the fired pellets are compared with those obtained from the plant data obtained in this research (Table 1) in order to assess the capability of the model. It is seen that the plant usage of fuel is slightly greater than that predicted by the simulated model. This seems to be due to the furnace leakage.

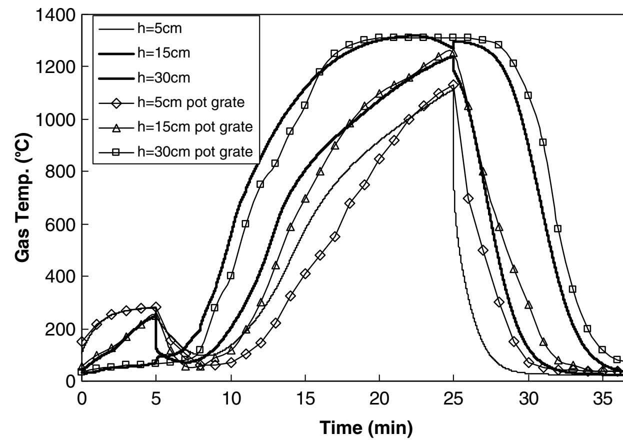

Fig. 2. Comparison of the simulation results (solid lines) with the experimental data obtained from pot grate measurements (dotted lines).

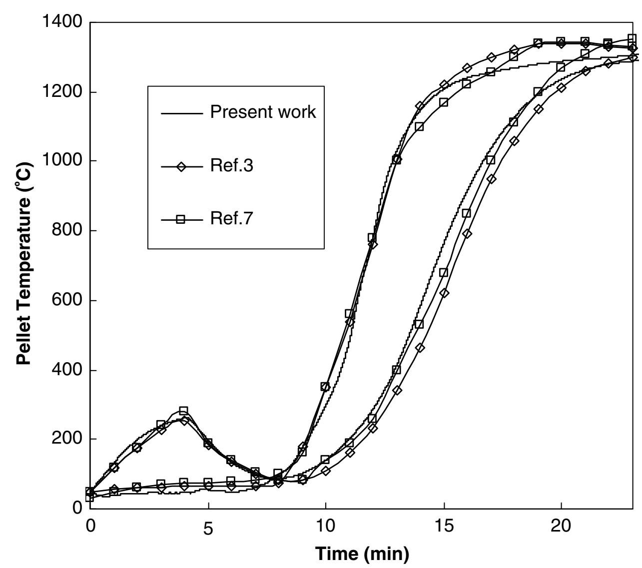

Fig. 3. Comparison of the temperature of the pellets calculated in this work with those of previous investigators [10,13].

Table 1
Comparison of the model data with those obtained from tests in the plant

Property	Plant	Model
N.G. consumption (Nm^3/ton)	20.87	20.05
Abrasion index	3.24	3.36

In order to study the possibility of the reduction of the fuel consumption with increasing of the productivity of the induration furnace by addition of carbon to the green pellets, six sets of conditions tabulated in Table 2 are utilized. Composition of green pellets is represented in Table 3. Different amounts of carbon added to the raw pellets are specified in Table 4. Pellets without carbon addition are categorized under Condition 1. Table 2 implies that an increscent in the carbon content of the pellets accompanies with increasing of the production rate by enhancement of the grate speed. In case of Condition 6, temperatures of the burner zones are decreased. Table 5 summarizes the specifications of the pellets in the grate bed.

Table 2
Carbon content of the green pellets and grate speeds

Condition	Carbon Content (%)	Grate Speed (m/min)
1	0	3
2	0.5	3.3
3	0.75	3.6
4	1.0	3.9
5	1.25	3.9
6	1.25	3.6

Table 3
Composition of green pellets

Constituent	Mass (%)
Fe_2O_3	63.6
Fe_3O_4	25.5
SiO_2	0.7
Al_2O_3	0.9
CaO	0.4
MgO	0.4
Moisture	8.5

Table 4
Burner zone temperatures

Burner Zone No.	Set Point Temperature (°C)	
	Conditions 1 to 5	Condition 6
1	840	840
2	860	860
3	1160	1100
4	1300	1170
5	1320	1180
6	1330	1200
7	1320	1180
8	1280	1050

Table 5
Specifications of the pellets in the bed

Hearth layer (cm)	10
Green pellet height (cm)	30
Void fraction of bed	0.39
Pellet diameter (cm)	1.2
Pellet porosity	0.30

Firing zones of the agglomeration plants are usually divided into several sections. These sections are called burner zones. This work focuses on pellettizing plant of Khouzestan Steel Company which has eight different burner zones. Separate control of the temperature in each burner zone is necessary. Other specifications of the plant are represented in Appendix 1. Set-points of all burner zones categorized under Conditions 1–5 are all the same. A lower temperature is used for the burner zones 3–8 of those under Condition 6. Specifications of the pellets used in KSC straight grate bed are demonstrated in Table 5.

Combustion of carbon in the pellets causes the formation of carbon monoxide and carbon dioxide, which heats up the pellets. As gas passes across the bed, its temperature increases. Fig. 4 shows the maximum temperature of the pellets that lay in height 11 cm from first layer of the green pellets. An increase in the temperature of the pellets causes the quality of the fired pellets to improve. Variation in the abrasion index of the fired pellets is illustrated in Fig. 5.

N.G. fuel consumption and electrical power utilization by the process can be decreased by adding carbon to the green pellets. Effect of carbon on N.G. fuel consumption and electrical power utilization are shown in Fig. 6. The effect of carbon content on the production rate of the straight grate is shown in Fig. 7. It is seen from these figures that adding 1% carbon to pellets can result in the following changes: (1) decrease of the fuel consumption by 24%, (2) increase of the production rate by 30% and (c) decrease of the electrical power by 23%.

Carbon contents of more than 1% may cause, however, exceeding of the pellet temperature from a critical value, T_C. The pellet quality may hence decrease due to the vitrification phenomenon described elsewhere [16]. Thermal profile of the pellets listed under Condition 5 (pellets having 1.25% carbon) is illustrated in

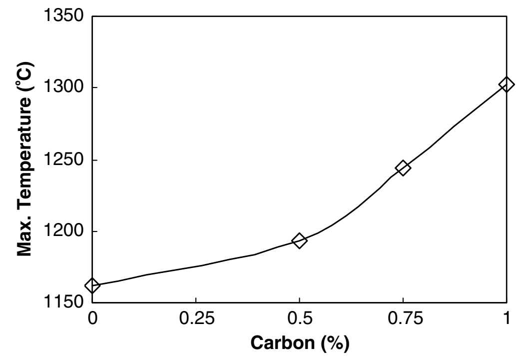

Fig. 4. Maximum temperature of the pellets that lay in height 11 cm from the first layer of the green pellets.

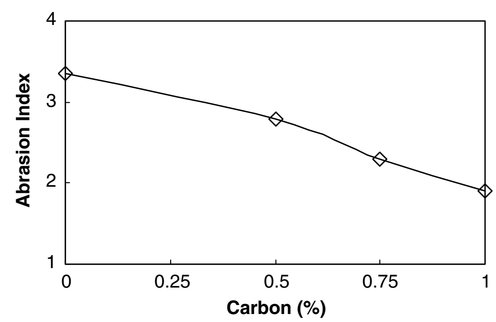

Fig. 5. Variation with carbon content of the abrasion index of the fired pellets.

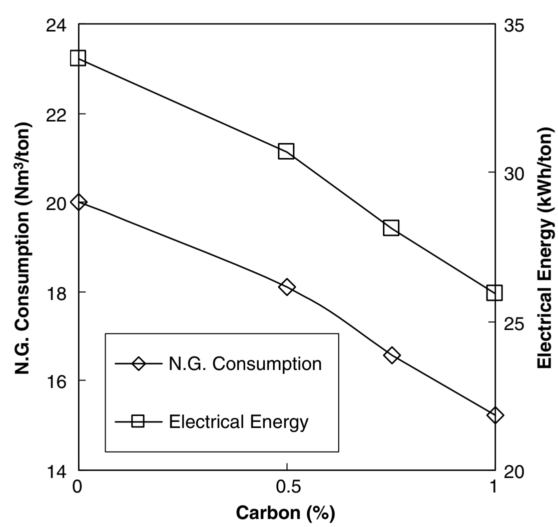

Fig. 6. Effects of the carbon content on the N.G. fuel consumption and the electrical power utilization in the induration process.

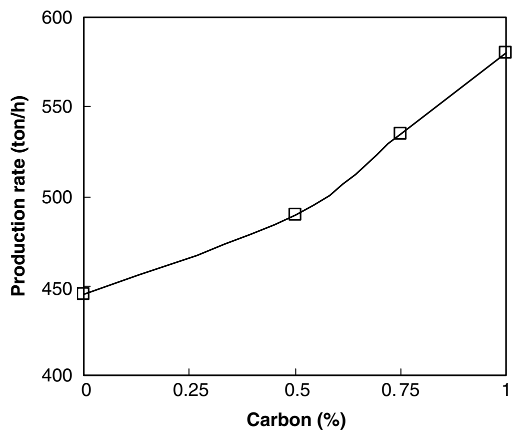

Fig. 7. Effect of the carbon content on the production rate of the induration process.

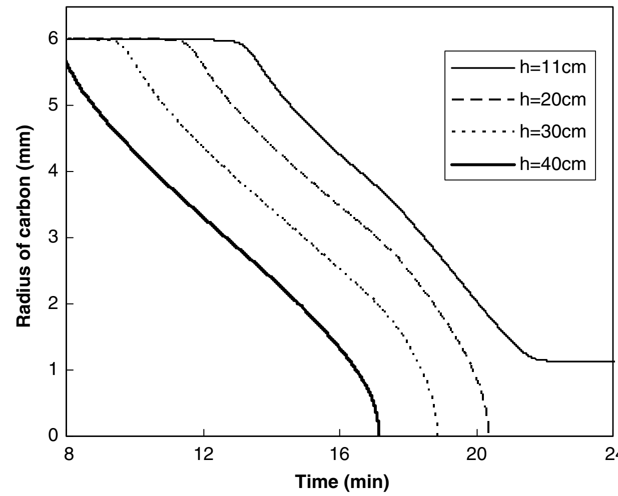

Fig. 9. Unreacted carbon remaining in the pellets under Condition 5.

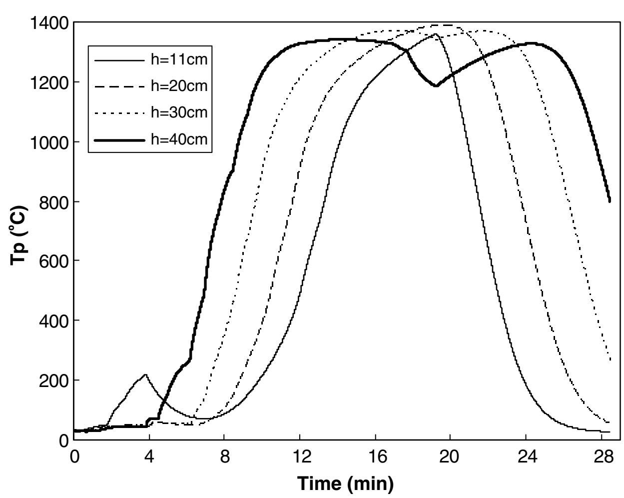

Fig. 8. Thermal profile of the pellets under Condition 5.

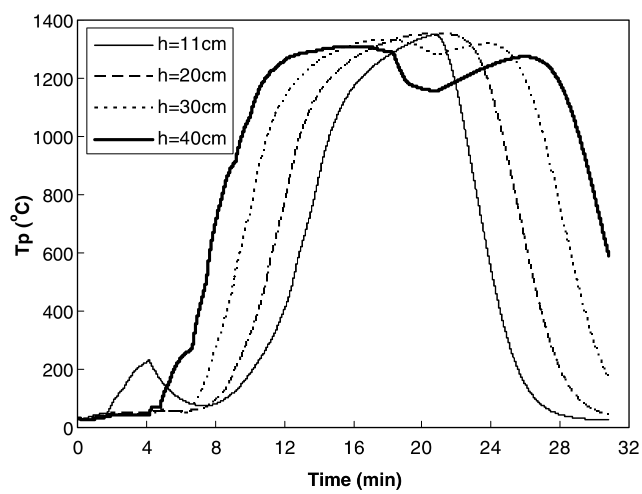

Fig. 10. Thermal profile of the pellets under Condition 6.

Fig. 8. As Fig. 8 shows, temperature of the pellets laid between the heights of 20 and 30 cm from the bottom of the bed exceeds 1360 °C. Mechanical properties of the fired pellets may, hence, worsen. This problem cannot be solved by increasing of the grate speed; because increasing of the grate speed can decrease the residence time of the pellets and increase their temperature further. This favors faster reaction of the remaining carbon and more heat production. This phenomenon is shown in Fig. 9 for Condition 5.

In order to overcome this problem, Condition 6 is considered to increase the process productivity. Under this condition, pellets containing 1.25% carbon ensures that carbon completely burns, grate speed decreases to 3.6 m/min. To avoid a too-high temperature rise, temperature of the burner zone decreases as stated in Table 5. Thermal profile of the pellets during induration process is illustrated in Fig. 10. Under this condition, in contrast to the pellets without carbon addition, temperature of the bottom layers exceeds those at the top. This is because of increasing of the gas temperature while rising across the bed. Grate bars may thus be burned. Fuel consumption of the process under this condition is 15.395 Nm^3/ton which is greater than that for Condition 4. It is concluded that increscent of the amount of carbon to more than 1% does not have desirable advantage.

It seems from the above discussion that in terms of the fuel consumption and product quality, the best result is obtained with pellets having 1% carbon content and grate speed equal to 3.9 m/min, but under these conditions because of the combustion of the carbon and the high grate-speed, residence time of the pellets in the cooling zones is not sufficient enough to keep the temperature at the safe value to protect the conveyer belts from undesirable damages. The length of the cooling zones must be increased to avoid the conveyer belts possible damages. The optimum content of the carbon is 0.75% with the present plant design of KSC. This result is in agreement with the experimental data of previous investigators [7]. Pellets having 0.75% carbon indicate a productivity increase of 20%, N.G. fuel consumption saving of 17.2% and electrical power decrease of 16.8% with respect to pellets with no carbon content.

Adding carbon to the pellets decreases the amount of the waste gases. Greenhouse gas generated in the induration process reduces hence due to the decreasing of the volume of the N.G. that burns in the process. It is seen that the carbon dioxide intensity trends are closely related to the energy intensity trends [20]. Fig. 11 compares the compositions of the gases that exit from the beds with Conditions 1 and 3. The changes are because of the decreasing of the N.G. which burns in preheating and firing zones of induration furnace which changes the carbon dioxide and water vapor emissions from the pellet production grate.

Effect of the addition of the carbon to the pellets on the volume of the waste gases that are produced in the induration process is

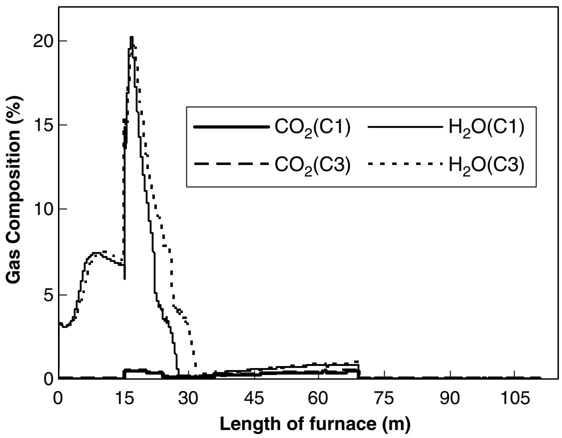

Fig. 11. Composition of the exhaust gases evolving from beds with Conditions 1 and 3.

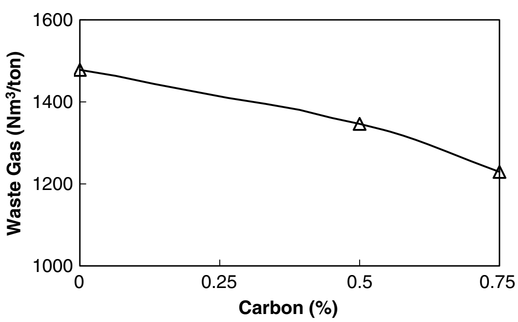

Fig. 12. Effect of carbon on the volume of the waste gases.

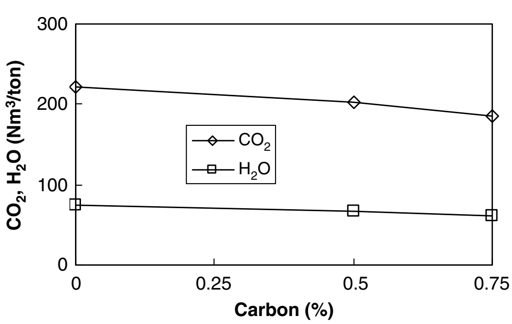

Fig. 13. Effect of carbon on the volume of the greenhouse gases.

Table A1
Number of wind boxes in each zone of an induration furnace located in KSC

Zone	UDD	DDD	PH	F1	F2	AF	C1	C2
Number of wind boxes	5	3	3	3	9	2	8	4

shown in Fig. 12. It is shown that under Condition 3 as compared to Condition 1, the volume of the waste gases decreases by 16.8%. Fig. 13 shows effect of carbon on the volume of the greenhouse gas concentrations that goes to stack.

The highly integrated nature of the pellets and the gas flow throughout the straight grate induration system means that small changes in the process conditions are reflected throughout the whole operation [4]. The main usefulness of the developed model over a range of the operating conditions should thus be in assessing of the fuel required to satisfactorily fire the system with model estimation of the heat distributed throughout the furnace. Although the model may be used to examine the effect of variation of the various parameters changing all together, the effect of addition of carbon to the raw pellets are discussed here.

4. Conclusion

The model developed in this investigation demonstrates that the induration process is very sensitive to the small changes in operational conditions. The effect of addition of carbon to the green pellets on the efficiency of the process is investigated from the perspective of fuel consumption, production rate and product quality. For any particular plant and pellet characteristics, there are a set of optimal furnace operational conditions and pellet carbon content. For KSC plants considered here, the best value of carbon is 0.75% which indicates an increased productivity of 20%, decreased N.G. fuel consumption of 17.2% and electrical power reduction of 16.8% with respect to the pellets with no carbon content.

Rising of the carbon content (for example by coke addition into the pellets), decreases the volume of the waste gases by 16.8% in the induration process. It also decreases the volume of the greenhouse gases per ton of the produced pellets and changes the composition of the waste gas evolving from the straight grate system.

Acknowledgements

The authors would like to acknowledge the Khouzestan Steel Company of Iran for financial support of the research and contribution of the plant data for assessment of the model.

Appendix 1

Characteristics of induration furnace: there are eight zones in each induration furnace of Khouzestan Steel Company (KSC). The bed of the pellets in the induration furnace is 3.3 m wide and 3 m long. Numbers of wind boxes in each zone are as indicated in Table A1.

References

[1] K. Meyer, Pelletizing of Iron Ores, Sprinter, Berlin, 1980.
[2] D. Pomerleau, A. Pomerleau, D. Hodouin, E. Poulin, Computers and Chemical Engineering 27 (2003) 217–233.
[3] J.A. Thurlby, Metallurgical Transaction B 19B (February) (1988) 122–132.
[4] R.J. Batterham, J.A. Thurlby, G.J. Thornton, The Chemical Engineer 55 (1977) 629–632.
[5] D. Pomerleau, A. Desbiens, D. Hodouin, Optimization of a simulated iron-oxide pellets induration furnace, in: 11th Mediterranean Conference on Control and Automation, 2003.
[6] M. Cross, P. Blot, Metallurgical and Materials Transactions B 30B (August) (1999) 803–813.
[7] A.A. Hamidi, H. Payab, IJE Transactions B 16 (3) (2003) 265–278.
[8] L. Price, J. Sinton, Energy 27 (2002) 426–429.
[9] N.A. Hasenack, P.A.M. Lebelle, J.J. Kooy, Induration process for pellets on a moving stand, in: Congress Proceedings Mathematical Process Models in Iron and Steelmaking, Metal Society, London (1975) 6–16.
[10] J.H. Voskamp, J. Brasz, Measurement and Control 8 (January) (1975).
[11] J.A. Thurlby, Metallurgical Transactions B 19B (February) (1988) 103–112.
[12] J.A. Thurlby, Metallurgical Transaction B 19B (February) (1988) 113–121.
[13] R.W. Young, M. Cross, R.D. Gibson, Ironmaking and Steelmaking 6 (1) (1979) 1–13.
[14] J.A. Thurlby, R.J. Batterham, R.E. Turner, International Journal of Mineral Processing 6 (6) (1979) 43–64.
[15] K. Kucukada, J. Thibault, D. Hodouin, G. Paquet, S. Caron, Canadian Metallurgical Quarterly 33 (1) (1994) 1–12.
[16] D. Pomerleau, D. Hodouin, E. Poulin, Canadian Metallurgical Quarterly 44 (4) (2005) 571–582.
[17] J. Mitterlehner, G. Loeffler, F. Winter, H. Hofbauer, H. Schmid, E. Zwittag, H. Buergler, O. Pammer, H. Stiasny;, ISIJ International 44 (1) (2004) 11–20.
[18] R.B. Bird, W.E. Stewart, E.N. Lightfoot, Transport Phenomena, John Wiley, New York, 2002.
[19] R.J. Battreham, Metallurgical Transactions B 17B (1986) 479–485.
[20] D. Cang, Y. Guan, H. Bai, Y. Zong, Y. Mao, X. Che, ISIJ International 42 (Supplement) (2002) S1–S4.